Indian Journal of Pure & Applied Physics
Vol. 52, February 2014, pp. 124-130

Structural and magnetic properties of $CuFe_2O_4$ as-prepared and thermally treated spinel nanoferrites

M Kanagaraj, P Sathishkumar, G Kalai Selvan, I Phebe Kokila & S Arumugam*

Centre for High Pressure Research, School of Physics, Bharathidasan University, Tiruchirappalli 620 024, Tamil Nadu, India

*E-mail: sarumugam1963@yahoo.com

Received 20 May 2013; revised 23 October 2013; accepted 26 November 2013

The copper based $CuFe_2O_4$ nanoferrite was prepared by chemical co-precipitation method and the detailed investigation of structural and magnetic properties was carried out successfully at room temperature. The obtained results from XRD confirm that $CuFe_2O_4$ has tetragonal structure at room temperature and its crystallite size, lattice strain was found to be varied from 11 to 17 nm and 3.9×10^{-2} to 2.6×10^{-2} for microwave annealed to as-prepared samples calculated using Scherrer equation and Williamson-Hall analysis, respectively. A clear superparamagnetic behaviour was observed in as-prepared and hot air oven annealed nanoferrite samples at RT under the field range of ±2 T. A distorted superparamagnetic curve was determined from isothermal magnetic hysteresis studies for the microwave oven annealed sample. It might be a possible magnetic and non-magnetic cation transformation on the surface of $CuFe_2O_4$ nanoparticles along with high lattice strain resulting in change of magnetic properties under certain level of applied magnetic field.

Keywords: Copper ferrite, Co-precipitation method, Microwave irradiation, Scherrer and Williamson-Hall analysis, Oxygen annealing, Superparamagnetism

1 Introduction

A peculiar improvement of spinel ferrites has been well realized in the field of electronics and communication for recent years[1]. Spinel type of $M^{2+}M_2^{3+}O_4$ structure has attracted much attention due to its chemical stability and various potential applications. In general, ferrites have a chemical formula[2,3] of MFe_2O_4 (M = Mn, Fe, Co, Ni, etc.). Among the many ferrites, $CuFe_2O_4$ cuprospinel has many advantages especially in gas sensor, hydrogen fabrication, proficient catalyst and superior magnetic and conducting properties. Most of the $CuFe_2O_4$ nanoferrite has inverse spinel structure at room temperature where eight (Cu^{2+}) are distributed on octahedral (B) sites and sixteen [Fe^{3+}(8)+Cu^{2+}(8)] ions share the tetrahedral (A) and octahedral (B) sites. There are numerous ways to bring nanometer sized particles; apart from that a chemical doping is one of the finest approaches, which leads to show a better crystalline size than by other methods[4,5]. Such ferrite nanoparticles have been synthesized through various bottom up approach techniques such as reverse micelle, chemical co-precipitation, microemulsion and sol-gel methods[6,7]. On comparing with conventional synthesis methods, chemical co-precipitation exhibits more merits and also it is very simpler technique by avoiding usages of large experimental setup with instruments.

In the case of nanoparticle fabrication, some other external factors are highly responsible for the modification of structure, transport and magnetic properties which are attributed to the type of synthesis methods. For example, excess of solvents, the presence of impurity phases and difficulty to control the ratio of oxygen content or oxygen deficiency, which could be adjusted by pursuing suitable heating treatments. It is also considered that the magnetic properties of spinel ferrites are very susceptible to cation and anion distribution with respect to temperature[8]. Because of short reaction time, high purity, simple and efficient energy transformation depends on the rate of nucleation growth by using microwave heating better than ordinary heating methods[9,10]. The synthesis and characterization of $CuFe_2O_4$ nanoparticles have been reported using chemical co-precipitation method and various heating for the same materials has also been carried out. The effect of crystallite size on the structural and magnetic properties with respect to different heating methods using hot air and microwave oven along with oxygen annealing at 700°C for six hours[11] has been investigated in the present paper.

2 Experimental Details

The high purity $CuCl_2.2H_2O$ (99.9% sigma Aldrich, India) and $FeCl_3$ (99.9% sigma Aldrich, India) were

used as starting materials. A mixed solution of one mole of $CuCl_2.2H_2O$ and two moles of $FeCl_3$ were continuously stirred and slowly heated at 60°C. Then, NaOH solution was added drop by drop and *p*H level is maintained within the range 10-12. Thereafter, the solution was allowed to cool down slowly with continuous stirring to room temperature. A few drops of polyethylene glycol (PEG) were added into the solution for the purpose of making homogeneous precipitation. Finally, the obtained precipitate was filtered and washed three times with hot distilled water, ethanol and once with acetone separately to remove sodium chloride and excess of surfactant present in the final precipitation. Then, half of the $CuFe_2O_4$ precipitate was taken into separate 50 ml beaker and it was placed in a microwave oven (Samsung, 750 W) for 10 min for drying. The remaining half of the sample was heated by hot air oven at 100°C for 6 h. At last, the dried brown $CuFe_2O_4$ powders from two different heating methods were subjected to thermal treatment such as oxygen annealing at 700°C using tubular furnace (VB ceramics, Ltd.).

The identification of phase and crystallite size of the as-prepared, Hot air Oven Annealed (HOA), and Microwave Oven Annealed (MOA) samples have been investigated using powder X-ray diffractometer (Rigaku Dmax/2C, Japan with Cu Kα radiation; α = 1.5405 Å). Surface morphology and existing compositions were analyzed by scanning electron microscopy (SEM; JEOL S-3000 Model) with EDAX spectrometer. The confirmation of functional groups present in all the samples was done by Fourier transform infrared spectroscopy (FTIR: Jasco460plus). Finally, the magnetic properties of as-prepared, HOA and MOA samples under applied magnetic field of ±1 Tesla were studied at room temperature (300 K) using Vibrating Sample Magnetometer (VSM) module (Lake Shore – 7474, USA).

3 Results and Discussion

The powder X-ray diffraction patterns of as-prepared, HOA, and MOA samples are shown in Fig. 1. All of the high intensity peaks are indexed and refined as tetragonal structure with $I4_1/amd$ space group, which is consistent with standard[12] JCPDS card no. 34-0425. The lattice parameters, unit cell volume, crystallite size and strain values were calculated using the following formulae given in Eqs (1-6).

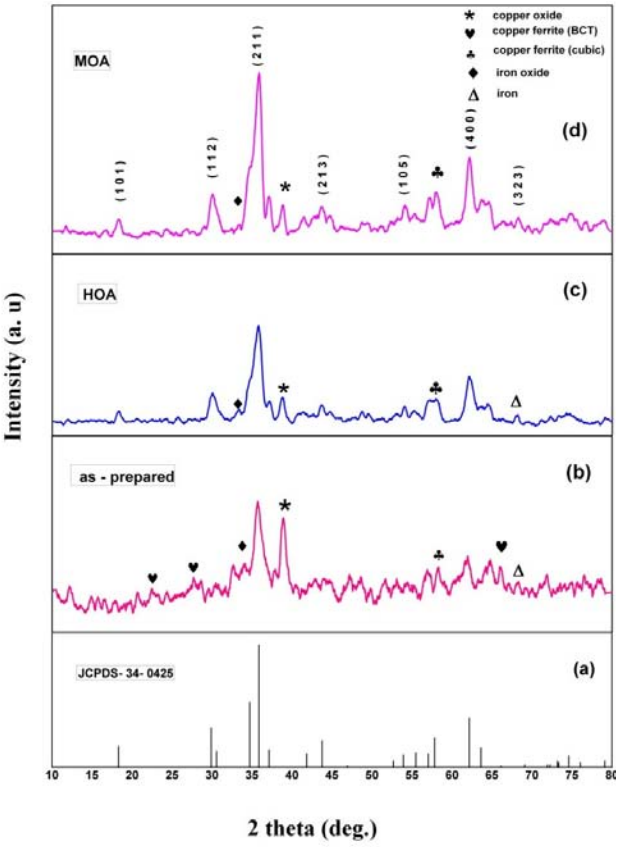

Fig. 1 — PXRD patterns of (a) standard $CuFe_2O_4$ JCPDS data, (b) as-prepared, (c) HOA and (d) MOA copper ferrite nanoparticles

$$\frac{1}{d^2}=\left(\frac{h^2}{a^2}\right)+\left(\frac{k^2}{a^2}+\frac{l^2}{c^2}\right) \quad ...(1)$$

$$V=a^2c \quad ...(2)$$

$$D=\frac{K\lambda}{\beta\cos\theta} \text{ (Scherrer's equation)} \quad ...(3)$$

$$\varepsilon=\frac{\beta_{hkl}}{4\tan\theta} \quad ...(4)$$

$$D=\frac{K\lambda}{(\beta\cos\theta-4\varepsilon\sin\theta)} \text{ (W-H equation)} \quad ...(5)$$

(or)

$$\beta\cos\theta=\frac{(k\lambda)}{(D)}+(4\varepsilon\sin\theta) \quad ...(6)$$

where K is the shape factor with a typical value of 0.9 in a spherical form, λ the X-ray wavelength (CuKα=1.540 Å), β the line broadening at half the

Table 1 — Comparison of structural characteristic parameters of as-prepared, HOA and MOA samples to standard JCPDS data

Samples	FWHM (Degree)	Particle Size (nm)	Crystallite size (nm) (S) method	Crystallite size (nm) (W-H) Method	Lattice parameters *a* (Å)	Lattice parameters *c* (Å)	*d* (Å)	*V*(m^3)
JCPDS (34-0425)	-	-	-	-	5.844	8.302	2.5069	294.79
as-prepared	0.495	68	26	17	5.922	8.792	2.5315	305.46
HOA[a]	0.596	51	21	14	5.811	8.648	2.5163	299.11
MOA[b]	0.743	66	18	11	5.860	8.592	2.5068	295.11

[a]Hot air Oven Annealed, [b] Microwave Oven Annealed

maximum intensity (FWHM) in radians and θ is the Bragg angle. From using Eq. (3) and FWHM on the peaks of (112), (211), (202) and (400), the crystallite size was found to be ~26, 21 and 18 nm for as-prepared, HOA and MOA samples, respectively. The comparison between structural parameters of as-prepared, HOA and MOA samples to $CuFe_2O_4$ standard JCPDS data are listed in Table 1. It is clearly seen that the value of crystallite size calculated from Scherrer's formula [Eq. (3)] is close to the values of Williamson-Hall equation and much lesser than the crystallite size values obtained in other synthesis methods[13,14]. The broadening of the observed X-ray peaks indicates that the obtained crystallite size is in nanometer range. However, some secondary phases of CuO, Fe_2O_3 and Fe_3O_4 were also found in as-prepared, MOA and HOA samples. The presence of such impurity phase might be due to the precipitation of Cu by PEG and insolubility[15] of FeO. The ferrite also has low temperature structural transition from tetragonal to cubic phase and swapping of several non-magnetic Cu^{2+} ions into (A) from (B) sites with respect to temperature[16].

The lattice parameter enhances with increase in grain size, which is in good agreement with the earlier observations of ferrites[17]. Figure 2 shows the relation between unit cell volume and strain with respect to crystallite size, which was calculated from Eqs (2) and (4). Eq. (4) represents the strain induced peak broadening with respect to imperfections and distortion in the sample. The distinct diffraction angle (θ) accounts for the dissociation of crystallite size and strain on peak broadening, which can be explained by Williamson and Hall equation or Uniform Deformation Model[18] (UDM). Using Eq. (6), we plot the βcosθ versus 4 sinθ and the linear fit was done by least square method as shown in Fig. 3. From *W-H* plot, we found the values of strain and crystallite size by the slope of linear curve and y-intersect of the linear fitted lines. In order to investigate the correlation between crystallite size and strain

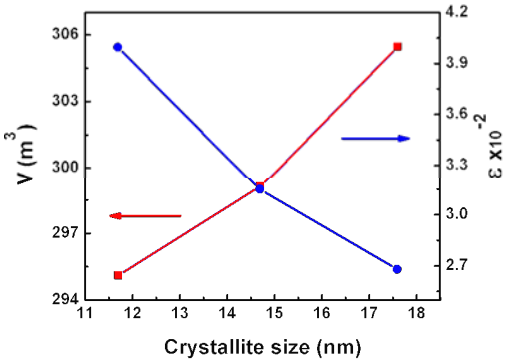

Fig. 2 — Correlation between volume (*V*) and strain (ε) with respect to crystallite size of $CuFe_2O_4$

calculated from *W-H* Eq. (5) and direct observation from *W-H* plot (Fig. 3), here we have listed all samples with crystallite size (*D*) and strain (ε) values in Table 2. As the crystallite size decreases the lattice strain tends to increase gradually and it may attribute to the reason for peak broadening. To compare with X-ray diffraction peaks and crystallite size of HOA, the MOA sample has a wide intensity peaks connected with single tetragonal phase, presence of minor impurity phases and reasonable lower crystallite size. It states that for synthesis of nanoparticles, microwave irradiation with suitable thermal treatment is better than other bottom up techniques as investigated so far[14].

The FTIR spectra recorded in the range 400-4000 cm^{-1} of as-prepared, HOA and MOA samples were shown in Fig. 4(a, b and c) and it confirm the presence of various functional groups in $CuFe_2O_4$. The vibration of ions in the crystal usually occurs while infra-red rays penetrate into the sample resulting transmittance was recorded in the form of IR spectrum[12]. Two main broad oxygen bands are clearly seen in the IR spectra of all spinels which correspond to the ferrite compounds. The observed FTIR spectrum of as-grown sample has two absorption bands at approximately 450-600 cm^{-1} and it is consisting of the octahedral (463.79 cm^{-1}) and

tetrahedral (580.46 cm^{-1}) sites of Cu cations in $CuFe_2O_4$. Waldron *et al*[19]. reported that the high absorption band found at ~ 546 cm^{-1} and 582 cm^{-1} accords to the intrinsic vibrations of tetrahedral complexes and lower absorption band at ~ 453 cm^{-1} and 437 cm^{-1} which might be attributed to the vibrations of octahedral complexes of HOA and MOA samples, respectively. The discrepancy between absorption peaks of octahedral and tetrahedral complexes in $CuFe_2O_4$ is due to the distance of Fe-O on octahedral and tetrahedral sites. The IR band value near 3840 cm^{-1} represents the existence of hydroxyl groups with vibrations (–OH). The other two peaks determined at approximately 2924-2921 cm^{-1} were assigned to the anti-symmetric and symmetric CH_2-vibrations of the carbon chains.

In Fig. 5(a, b and c), we have shown the SEM micrographs of $CuFe_2O_4$ powders synthesized by co-precipitation method. This technique is mainly used to see the surface morphology and distribution of synthesized particles lying in the micro to nano level. It is noted that the shape of $CuFe_2O_4$ powder obtained from precipitation method seems to be strongly agglomerated and some tiny fraction of plate like

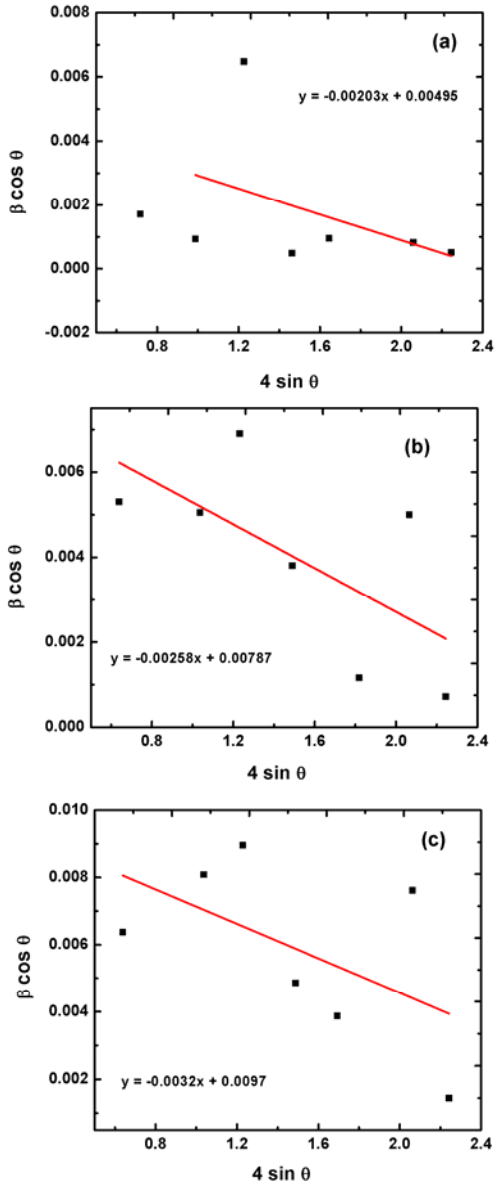

Fig. 3 — *W – H* plots for (a) as-prepared, (b) HOA, and (c) MOA $CuFe_2O_4$. For fitting Eq. (6), (β cosθ versus 4 sinθ) the strain and crystallite size have been calculated from the slope and y-intercept of the linear fitted curves.

Table 2 — Geometrical factors and its comparison of $CuFe_2O_4$ as-prepared, HOA and MOA samples

Samples	Crystallite size (*D*) in nm		Lattice strain (ε)	
	W-H equation	W-H plot	W-H equation (10^{-2})	W-H Plot (10^{-3})
as-prepared	17	28	2.680	2.03
HOA	14	17	3.150	2.58
MOA	11	14	3.996	3.20

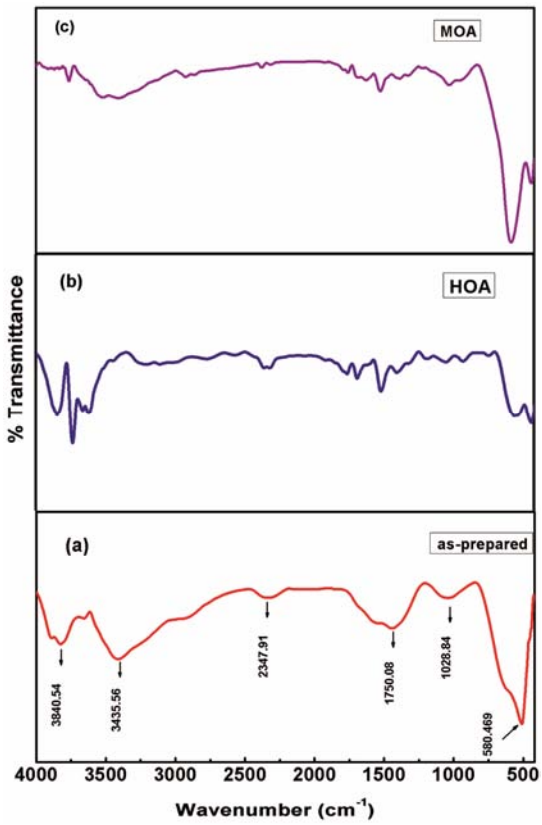

Fig. 4 — FTIR spectrum of (a) as-prepared, (b) HOA and (c) MOA cuprospinel nanoparticles

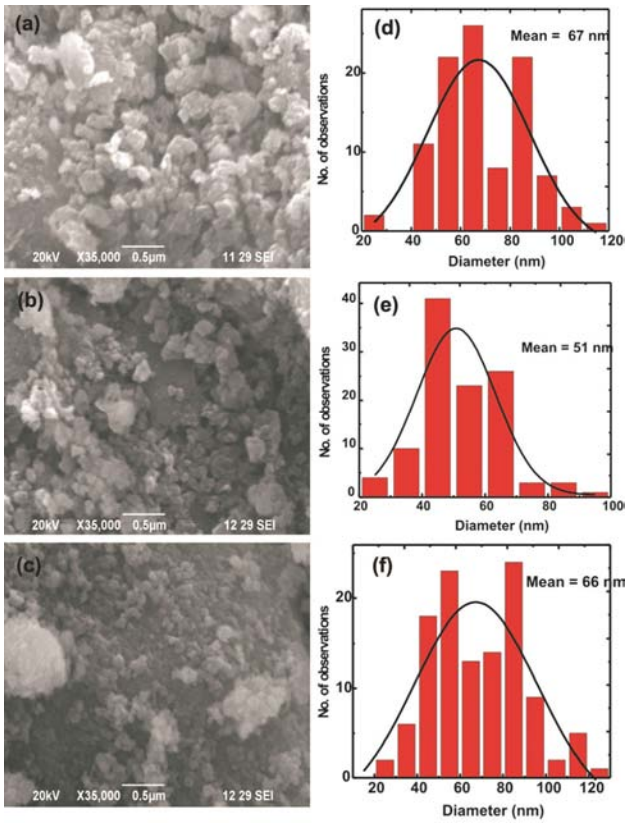

Fig. 5 — (a-c) SEM micrographs and (d-f) particles distribution of the as-prepared, HOA and MOA samples

grains were also seen in the SEM picture. However, the reason for the resultant large grain size distribution might be related to grain growth conditions and densification of the crystallites[12]. The particle size calculated for all the three samples from SEM pictures and through image j software was found to be within the range 50 ± 20 nm, which is illustrated in Fig. 5(d, e and f). The EDAX analysis based on the strength of the emission energies of the characteristic elements were also investigated. Since, we are interested in the investigation of MOA sample with existing elements and so here we have taken EDAX spectrum as shown in Fig. 6. It supports the presence of Cu, Fe, and O elements in the final $CuFe_2O_4$ and thus deviation from the initial stoichiometry values as shown in the Fig. 6 with inset Table. The maximum intensity was found in Fe atom and second, third minimum intensity peaks represent O and Cu atoms. This spectrum provides the final confirmation of $CuFe_2O_4$ nanoparticles synthesized by co-precipitation techniques and it does not show any other impurity elements in the existing sample. Fig. 6 with inset clearly shows atomic and weight

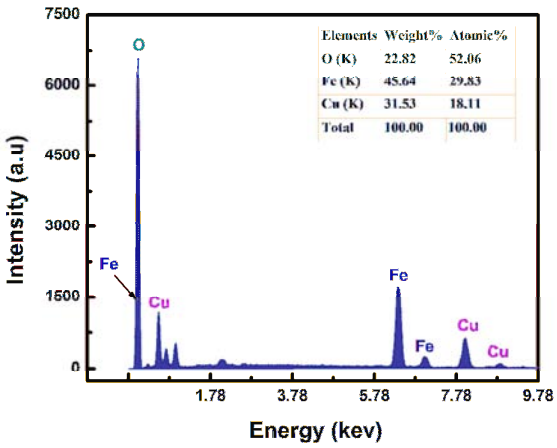

Fig. 6 — EDAX spectra for $CuFe_2O_4$ sample

percentage of $CuFe_2O_4$ with corresponding stoichiometry values of the existing Fe, Cu, and O elements.

The magnetic field dependence of magnetization at room temperature was carried out using vibrating sample magnetometer in the applied field range of ± 20 kOe for as-prepared, HOA and MOA samples as shown in Fig. 7(a). It demonstrates hysteresis of as-prepared and HOA samples having perfect "S" shaped superparamagnetic curves at room temperature, which are characteristic of magnetic property of nanocrystalline materials because of their small crystallite size[5,14,15,20]. From that hysteresis curves, the saturation magnetization (M_s), remanent magnetization (M_r) and coercive field were found to be M_s = 15.26, 9.27 and 2.177 (emu/g), M_r = 1.51, 0.32 and 0.05 (emu/g), and H_c = 101.86, 41.07 and 23.32 (Oe) for as-prepared, HOA and MOA samples, respectively. For nanomaterials, the most important postulate to consider is that the correlation between core and shell atoms with interaction should significantly change their magnetic and electrical properties. However, the relation between crystallite size and spin order of the existing elements on the surface is one of the predominant factor, which directly responds to the magnetic property of nanocrystallites. For that reason, here we have tabulated and compared the crystallite size and change of M_s, H_c and M_r in Table 3. Fig. 7(b) shows the coercivity (H_c) and the ratio of remnant magnetization to saturation magnetization (M_r/M_s) as a function of different crystallite size. It should be noted that with decreasing crystallite size, the values of H_c and M_r also decrease and this correspond to the affirmation of superparamagnetic (SP) behaviour present at room temperature for as grown and HOA samples of

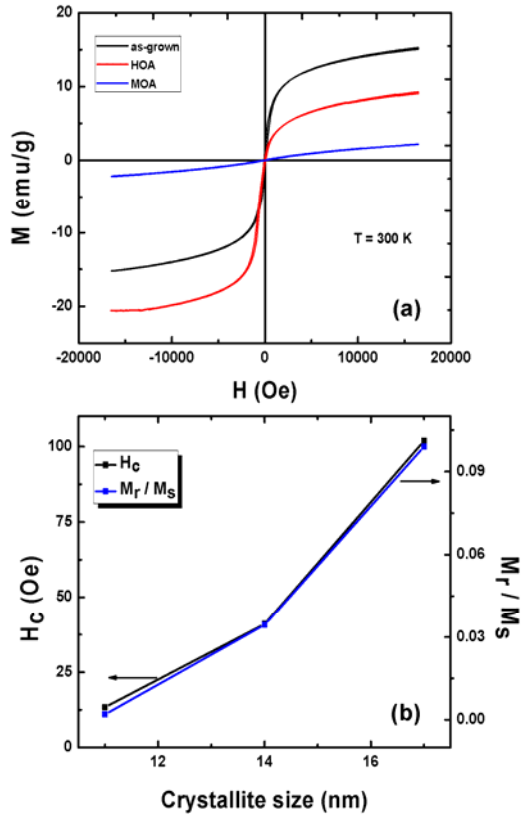

Fig. 7 — (a) Hysteresis curves for as-prepared, HOA and MOA $CuFe_2O_4$ at room temperature under magnetic field of ± 20000 Oe and (b) Crystallite size depends on coercivity (H_c) and remanent magnetization to saturation magnetization ratio (M_r/M_s) of the same samples

$CuFe_2O_4$. A similar characteristic has also been observed for many spinel ferrites at room temperature[13,15].

From Fig. 7(a) and the values of M_s, M_r and M_r/M_s ratio of MOA sample strongly deviate from "S" shaped superparamagnetic curve (SP state), which can be clearly seen from very low H_c and M_r/M_s values with respect to crystallite size as shown in Fig. 7(b). Under thermal treatment such as annealing, it enhances the reordering of Cu^{2+} (non-magnetic) and Fe^{3+} (ferromagnetic) atoms, which were located in octahedral and tetrahedral sites. Most spinel ferrites have cubic structure at room temperature, though there are some remonstrations that $CuFe_2O_4$ would have a tetragonal or distorted tetragonal phase while undergoing thermal treatments[14,20-22]. The M_r and M_r/M_s of MOA sample are much less than other as-prepared and HOA $CuFe_2O_4$ samples. There are two possible reasons for this specific magnetic contest: (1) the observed XRD peaks of MOA sample reveal the presence of strong magnetic impurity (Fe_2O_3) and

Table 3 — Effect of crystallite size on the magnetic properties of as-prepared and thermally treated cuprospinel ferrites

Samples	Crystallite size (nm)	Saturation magnetization M_s (emu/g)	Coercivity H_c (Oe)	Remanent magnetization M_r (emu/g)	M_r/M_s
as-prepared	17	15.26	101.86	1.51	0.099
HOA	14	9.27	41.07	0.32	0.034
MOA	11	2.17	13.32	0.005	0.002

it is suppressed when annealing at 700°C under oxygen atmosphere. Since, a weak ferromagnetic (or) strong paramagnetic nature will arise if ferromagnetic impurity is suppressed as well as due to reduction of crystallite size by thermal process. In addition, there is a possibility of transferring Fe^{3+} cations into non-magnetic octahedral (B) sites in the spinel lattices resulting in drastic variation of M_s between as-prepared and MOA samples. (2) The presence of other parameters like lattice strain (ε) and magnetic crystalline anisotropy under high magnetic field could break the number of ferromagnetic domains and thus reduce the magnetization energy [23,24]. Obviously, when reducing crystallite size from 17 nm to 11 nm for as-prepared to MOA samples (Table 2), the H_c, M_r and M_r/M_s factors have to decrease, and nevertheless it enhances the lattice strain from 2.6×10^{-2} to 3.9×10^{-2}. In our case, MOA sample shows a distorted paramagnetic state, which might be a magnetic cations distribution or deformation on the surface of core atom with spin orders and increasing strain, sometimes both play an important role for change of magnetic property at room temperature in $CuFe_2O_4$ spinel ferrites.

4 Conclusions

In summary, $CuFe_2O_4$ nanoferrites were synthesized by a simple chemical co-precipitation method and the resulting powder was subjected to hot air and microwave heating in order to remove the excess of solvent and impurities. Use of thermal treatment under oxygen atmosphere at 700°C further gives better crystallinity. From a detailed investigation of XRD, the mean crystallite size was found to decrease from 17 nm to 11 nm and lattice strain enhances 2.6×10^{-2} to 3.9×10^{-2} for as-prepared to MOA samples, respectively. It is comparatively closer to direct observation of *W-H* plots with crystallite size and strain values. Other studies with results such as FTIR and SEM with EDAX confirm the presence of major $CuFe_2O_4$ peaks with

corresponding band assignments. At room temperature, magnetic hysteresis studies show a significant discrepancy between as-prepared and MOA samples with respect to applied external magnetic field. The observed M versus H curves of as-prepared and HOA samples reveal a perfect superparamagnetic behaviour at room temperature and other related factors M_s, M_r and M_r/M_s ratio decrease while reducing crystallite size, which is a predominant characteristic of magnetic properties of ferrite nanoparticles. However, MOA ferrite has a large deviation from SP state in other words it has a strong paramagnetic nature even at low magnetic field when compared with other ferrites. This might be magnetic cations (Fe^{3+}) transferring into non-magnetic octahedral (B) sites by oxygen annealing or due to high lattice strain. Other reason could be increase in magnetic crystalline anisotropy of magnetic cations on the surface of nanoparticles under high magnetic field, which is eventually brought to distorted paramagnetic state at room temperature.

Acknowledgement

The authors wish to thank DST, SERC, IDP, FIST and UGC, New Delhi for the financial support of this research work. The author M Kanagaraj thanks CSIR for fellowship. G Kalai Selvan would like to thank UGC-BSR for the meritorious fellowship.

References

1 Pradeep A & Thangasamy C, *J Mater Sci & Electronics*, 15 (2004) 797.
2 Sugimoto M, *J Am Ceram Soc,* 82 (1999) 269.
3 Satyanarayana L, Reddy K M & Sunkara V M, *Mater Chem Phys*, 82 (2003) 21.
4 Ludwig F, Guillaume A, Schilling M, Frickel N & Schmidt A M, *J Appl Phys*, 108 (2010) 033918.
5 Kalai Selvan R, Augustin C O, Sanjeeviraja C & Prabhakaran D, *Solid State Commun*, 137 (2006) 512.
6 Popescu S A, Valzan P, Notingher P V, Novaconi S, Grozescu I & Sfirloaga P, *Optoelectron Adv Mat*, 13 (2011) 2-4 (260).
7 Rus S F, Vlazan P, Novaconi S, Grozescu I & Sfirloaga P, *Optoelectron Adv Mat*, 14 (2012) 3-4 (293).
8 Pajic D, Zadro K, Vanderberghe R E & Nedkov I, *J Mag Magn Mater*, 281 (2004) 353.
9 Rao K J, Vaidhyanathan B, Gaguli M & Ramakrishnan P A, *Chem Mater*, 11 (1999) 882.
10 Wang H, Xu J Z, Zhu J J & Chen H Y, *J Cryst Growth*, 244 (2002) 88.
11 Faraji M, Yamini Y, Rezaee M & Iran J, *Chem Soc*, 7 (2010) 1 (1-37).
12 Ponhan W & Maensiri S, *Solid State Sci*, 11 (2009) 479.
13 Chia C H, Zakaria S, Yusoff M, Goh S C, Haw C Y, Ahmadi S, Huang N M & Lim H N, *Ceram Intern*, 36 (2010) 605.
14 Laokul P, Amornkitbamrung V, Seraphin S, & Maensiri S, *Current Appl Phys*, 11 (2011) 101-108.
15 Ahmed Y M Z, Hessien M M, Rashad M M & Ibrahim I A, *J Magn Magn Mater*, 321 (2009) 181.
16 Nedkov I, Merodiiska T, Milenova L & Koutzarova T, *J Magn Magn Mater*, 211 (2000) 296.
17 Pan W, Gu F, Qi K, Liu Q & Wang J, *Mater Chem Phys*, 134 (2012) 1097.
18 Zak A K, Majid W H A, Abrishami M E & Yousefi R, *Solid State Sci*, 13 (2011) 251.
19 Waldron R D, *Phys Rev*, 99 (1955) 1727.
20 Stewart S J, Tueros M J, Cernicchiaro G & Scorzelli R B, *Solid State Commun*, 129 (2004) 347.
21 Kang K S, Kim C H, Cho W C, wang Bae K K, Woo S W & Park C S, *International Journal of hydrogen energy,* 33 (2008) 4560-4568.
22 Chen H, Yang S, Chang Y, Yu K, Li D, Sun C & Li A, *Chemoshpere*, 89 (2012) 185.
23 Anjaneyulu T, Narayana Murthy P, Narendra K & Vijaya Kumar K, *International Journal of Basic and Applied Chemical Sciences,* 3 (2013), 50-59.
24 Naseri M G, Saion E B, Ahangar H A, Hashim M & Shaari A H, *Powder Technology*, 212 (2011) 80